

Gamow-Teller strength from the $^{76}\text{Se}(n,p)^{76}\text{As}$ reaction: Implications for the double β decay of ^{76}Ge

R. L. Helmer,^{1,2} M. A. Punyasena,³ R. Abegg,² W. P. Alford,¹ A. Celler,⁴ S. El-Kateb,⁵ J. Engel,^{6,*} D. Frekers,²
R. S. Henderson,^{2,7} K. P. Jackson,² S. Long,⁷ C. A. Miller,² W. C. Olsen,³ B. M. Spicer,⁷
A. Trudel,⁴ and M. C. Vetterli²

¹University of Western Ontario, London, Ontario, Canada N6A 3K7

²TRIUMF, 4004 Wesbrook Mall, Vancouver, British Columbia, Canada V6T 2A3

³University of Alberta, Edmonton, Alberta, Canada T6G 2N5

⁴Simon Fraser University, Burnaby, British Columbia, Canada V5A 1S6

⁵King Fahd University of Petroleum and Minerals, Dhahran, Saudi Arabia

⁶California Institute of Technology, Pasadena, California

⁷University of Melbourne, Parkville, Victoria 3052, Australia

(Received 19 September 1996)

Cross sections have been measured up to 35 MeV excitation for the $^{76}\text{Se}(n,p)^{76}\text{As}$ reaction at five laboratory angles between 0° and 15° . The incident neutron energy was 198 MeV. The distribution of Gamow-Teller (GT) strength at excitation energies less than 10 MeV was deduced by carrying out a multipole decomposition of the data. The GT strength below 6 MeV excitation was found to be less than 0.9 units, in qualitative agreement with a quasiparticle random-phase approximation calculation. The present results have been compared with data from the $^{76}\text{Ge}(p,n)^{76}\text{As}$ reaction to obtain an estimate of a lower limit for the lifetime of ^{76}Ge for $\beta\beta$ decay. The estimate is in qualitative agreement with the measured lifetime. [S0556-2813(97)03206-8]

PACS number(s): 25.40.Kv, 24.30.Cz, 27.50.+e, 23.40.-s

I. INTRODUCTION

At bombarding energies between 200 and 300 MeV, it has been found that the $\Delta L=0$, $\Delta J^\pi=1^+$ spin-flip isovector excitation (Gamow-Teller) dominates over the $\Delta J^\pi=0^+$ non-spin-flip (Fermi) component of the nucleon-nucleon effective interaction [1,2]. It has also been shown that 0° cross sections measured in both (p,n) [3] and (n,p) [4] reactions, extrapolated to zero momentum transfer, are proportional to the Gamow-Teller (GT) beta decay (β -decay) strength between the same initial and final states [5]. Therefore, these reactions are ideal probes of GT strength, especially in cases not energetically accessible in ordinary β decay, and indeed they have been exploited to measure the distribution of GT β -decay strength in a wide range of nuclei [1–18].

The distribution is of particular interest for transitions between the intermediate states involved in nuclear double beta decay ($\beta\beta$ decay) and the respective initial and final states. Double β decay with two neutrinos in the final state ($2\nu\beta\beta$ decay) is an allowed second-order weak process which has now been observed or inferred for a number of nuclei [19–26], while that with no neutrinos in the final state ($0\nu\beta\beta$ decay) is a lepton number violating process forbidden in the standard model. Apart from the intrinsic interest in observing such weak reactions, $0\nu\beta\beta$ decay is also of interest because it has been shown that the rate of the decay can be related to a nonzero mass for the neutrino, and hence provides a glimpse of possible physics beyond the standard

model. For the more common 2ν mode, the $\beta\beta$ -decay rate is given by [27]

$$\lambda_{2\nu} = f_{2\nu} |M_{2\nu}|^2, \quad (1)$$

where $f_{2\nu}$ is a phase-space factor. The nuclear matrix element is given by [28]

$$M_{2\nu} = \sum_m \frac{\langle f || t_- \sigma || m \rangle \langle m || t_- \sigma || i \rangle}{E_{xm} + \Delta M + \frac{1}{2} T_0}, \quad (2)$$

where $t_- \sigma$ is the Gamow-Teller operator connecting the initial and final $J^\pi=0^+$ states with intermediate $J^\pi=1^+$ states, T_0 is the energy released in the decay, ΔM is the atomic mass difference between the initial and intermediate nuclei, and E_{xm} are the excitation energies of the intermediate states.

For $0\nu\beta\beta$ decay, a similar expression holds [27]

$$\lambda_{0\nu} = f_{0\nu} |M_{0\nu}|^2 \left[\frac{m_\nu}{m_e} \right]^2, \quad (3)$$

where again $f_{0\nu}$ is a phase-space factor, and m_ν is the putative neutrino mass (in units of the electron rest mass). In this case the nuclear matrix element, $M_{0\nu}$, is identical in form to the matrix element in the two neutrino case,

$$M_{0\nu} = \sum_m \frac{\langle f || t_- \sigma || m \rangle \langle m || t_- \sigma || i \rangle}{E_{xm} + \Delta M + \frac{1}{2} T_0}, \quad (4)$$

but the summation now runs over intermediate states of all spins and parities. An estimate of $M_{0\nu}$ is clearly a prerequisite for relating a lifetime measured in $0\nu\beta\beta$ decay to a

*Present address: Department of Physics and Astronomy, CB3255, University of North Carolina, Chapel Hill, NC 27599.

neutrino mass, or in the event the decay is not observed, for establishing a limit on the mass from a limit on the lifetime.

One of the difficulties that had to be overcome before calculations of these matrix elements could be considered reliable was that even in the simpler case of $2\nu\beta\beta$ decay where only 1^+ intermediate states are excited, it proved to be very difficult to calculate rates that were consistent with measured values. Early shell-model calculations for this mode overestimated the rate of decay, typically by up to two orders of magnitude [27]. Eventually it was found, within the context of the quasiparticle random-phase approximation (QRPA), that deuteronlike particle-particle correlations in the nuclear ground state dramatically reduce the $2\nu\beta\beta$ -decay rates [29]. Recent QRPA calculations incorporating particle-particle forces have been in quantitative agreement with measured rates [30,31].

A by-product of the QRPA calculations is that the spectrum of intermediate 1^+ states is explicitly determined. Therefore, in addition to comparison with measured $\beta\beta$ -decay rates, a detailed test of the nuclear wave functions can be made by comparing the calculated spectra with the spectra measured in (p,n) and (n,p) reactions [32]. Note that the second factor of each term in the sum for $M_{2\nu}$ [see Eq. (2)], is the matrix element for GT β^- transitions between the initial state and the corresponding 1^+ state in the intermediate nucleus. As noted above (see also Ref. [33]) both the β -decay strength and cross section of the (p,n) reaction between these states are proportional to the square of this matrix element. Similarly, the (n,p) cross section for the transition between the ground state of the final nucleus and the intermediate 1^+ states is proportional to the square of the first matrix element in Eq. (2).

In the experiment described here, the GT strength is deduced for the $^{76}\text{Se}(n,p)^{76}\text{As}$ reaction. The data can therefore provide a useful test of wave functions used in calculations of decay rates for this nucleus. A study of the $^{48}\text{Ti}(n,p)^{48}\text{Sc}$ reaction which is relevant to the $\beta\beta$ decay of ^{48}Ca has also been reported [12]. In this case it was found that both shell-model [28,34] and QRPA [12] calculations gave a rather poor fit to the measured GT strength.

II. EXPERIMENTAL MEASUREMENTS

The experiment was carried out using the TRIUMF charge exchange facility in the (n,p) mode. The operation of this facility is described in detail elsewhere [35]; here a brief description relevant to the present measurements is given. A schematic view of the facility is shown in Fig. 1.

Protons of 200 MeV kinetic energy are directed onto a 240 mg/cm^2 thick foil of ^7Li , and then are bent by a sweeping magnet into a shielded beam dump. Nearly monoenergetic neutrons from the $^7\text{Li}(p,n)^7\text{Be}$ reaction impinge on the ^{76}Se targets contained in a target box [36] located over the pivot of a medium resolution spectrometer (MRS) [37]. The box has provision for up to six targets, each of which is mounted between proportional wire chambers. From the pattern of hits on the wire chamber planes, it is possible to identify the target in which the (n,p) reaction occurs. An energy-loss correction can then be applied for protons traversing the material downstream from the struck target, making it possible to maintain satisfactory energy resolution

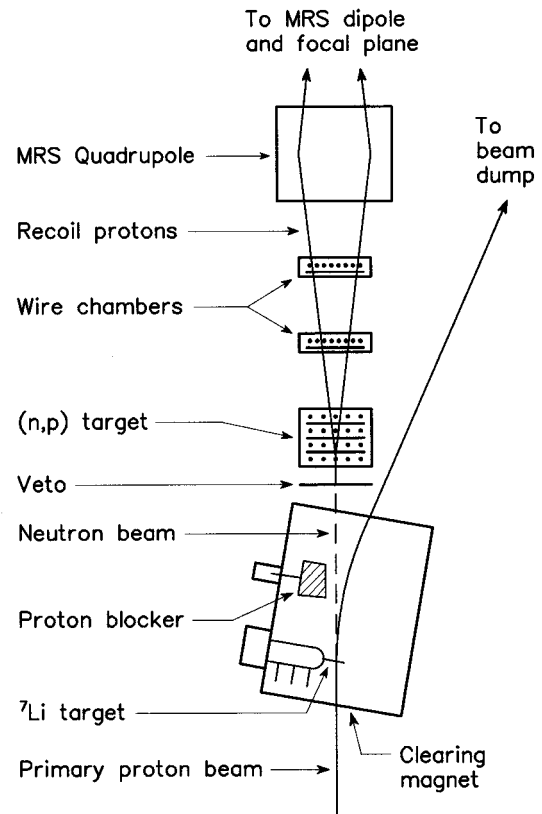


FIG. 1. Schematic view of the TRIUMF charge exchange facility in (n,p) mode. The neutron beam is produced by the $^7\text{Li}(p,n)^7\text{Be}$ reaction. Protons from (n,p) reactions in the secondary target are detected in the MRS. The proton beam is deflected into a beam dump after passing through the primary target.

even for quite thick targets, up to $\approx 1\text{ g/cm}^2$. Protons from (n,p) reactions in the target material are momentum analyzed and detected with the MRS. The transverse positions of their origins in the target material is determined by tracing back their tracks through two multiwire chambers located between the target box and the MRS. In this way protons originating from outside the area of the target material can be removed from the data set. Charged particles incident on the target box are vetoed by a thin scintillator just upstream from the box and by two wire planes just after its entrance window.

Four selenium targets were mounted in the target box. Each consisted of a powder (enriched to 96.9% ^{76}Se , obtained from ORNL) sandwiched between Mylar foils glued to copper frames. The inside dimensions of each frame were $2.2\text{ cm} \times 4\text{ cm}$, and the average selenium thickness of each target was 282 mg/cm^2 . The last target in the stack was a 46.7 mg/cm^2 thick CH_2 foil, used to normalize the $\text{Se}(n,p)$ cross section to the known $\text{H}(n,p)$ cross section [38].

Spectra were measured up to 35 MeV excitation at MRS angles of 0° , 3° , 6° , 10° , and 15° . Data were recorded event-by-event and written to magnetic tape for later off-line analysis. A fraction of the events was analyzed on-line to monitor the progress of the experiment.

A subsidiary measurement with six CH_2 targets in the box, each with nominal thickness 140 mg/cm^2 , was taken at

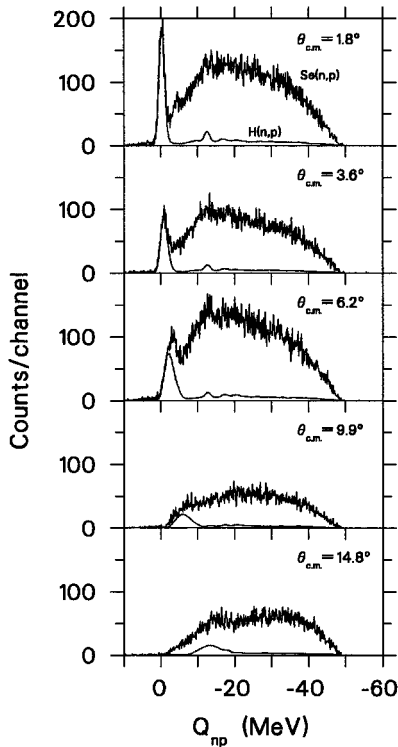


FIG. 2. Raw spectra for the five angle settings of the MRS. The sum of the data from the four selenium targets, and the data from the CH_2 target at the end of the selenium target stack, are shown. Corrections have been applied to account for the different energy losses suffered by protons originating in the different target layers, and for aberrations associated with the MRS.

a spectrometer angle of 0° . These data were used to establish the energy calibration and the focal plane acceptance of the MRS. For these measurements, the peak from the $\text{H}(n,p)$ reaction was stepped across the focal plane by varying the magnetic field of the spectrometer. Normalization among the various runs for the acceptance data was achieved by integrating the charge collected in a Faraday cup in the beam dump.

Finally, data were also collected with a target stack identical to the one used for the selenium targets, except that no material was contained between the Mylar foils. In principle, these data could be used for background subtraction, but in practice the data came in too slowly for this to be practical. It was found that a satisfactory background subtraction could be made by using the spectrum from the CH_2 target at the end of the stack of selenium targets. The empty target runs were then used just to ensure that no significant unexpected source of background was present.

III. DATA ANALYSIS

Raw spectra for the sums of the data from the selenium targets are shown in Fig. 2. The angles shown are the scattering angles averaged over the $\pm 2^\circ$ acceptance of the MRS, converted to the center of mass. The data have been corrected for the different energy losses suffered by protons from interactions in the different target layers, and for aberrations associated with the MRS. The procedures for apply-

ing these corrections are described elsewhere [35]. The forward angle spectra show a pronounced peak at low excitation arising from the $^1\text{H}(n,p)$ reaction on hydrogen in the Mylar foils of the targets and the wire chamber planes, and possibly from water vapor adsorbed on various surfaces.

The spectrum from the CH_2 target used for background subtraction is also shown in Fig. 2. The normalization for the subtraction was fixed for all the angles by requiring complete elimination of the $\text{H}(n,p)$ peak from the $\text{Se}(n,p)$ spectrum at 0° . At this angle, there should be few events from the $^{76}\text{Se}(n,p)^{76}\text{As}$ reaction under the hydrogen peak [the ground-state Q value for $^{76}\text{Se}(n,p)$ is -2.185 MeV]. It can be seen in Fig. 2 how the hydrogen peak is kinematically shifted and broadened as the MRS angle is increased, and the resulting mixing of events from the two reactions otherwise makes it difficult to establish a normalization at the other angles.

It should be noted that the actual sources of background have a different C to H ratio than the CH_2 target, and they happen to be present in such proportion that there is a slight oversubtraction in the region of the peak from the $^{12}\text{C}(n,p)^{12}\text{B}$ reaction at $Q = -12.6$ MeV. Nevertheless, the difference between the CH_2 spectra and the true background is less than the statistical uncertainty in the data and was consequently neglected. In fact, except for the region around the hydrogen peaks, the subtraction has little significant effect on the spectra.

It can also be determined from the $\text{H}(n,p)$ peak in the 0° spectrum that the overall energy resolution is about 1.8 MeV [full width at half maximum (FWHM)]. The main contributions to the energy resolution are the energy spread of the primary proton beam (≈ 1 MeV), the energy loss in the ^7Li target (≈ 870 keV), the $^7\text{Li}(p,n)$ reaction populating about equally both the ground state and 430 keV first excited state of ^7Be , and the energy loss and straggling in the selenium targets in the target stack. The energy losses of the four selenium targets were calculated to be 831, 807, 792, and 841 keV.

The spectra with the background subtracted and the data summed into 1 MeV wide bins are shown in Fig. 3. In addition to the corrections applied to the spectra shown in Fig. 2, the spectra in Fig. 3 have been corrected for the variation of the MRS focal plane acceptance and for the effects of a weak continuum in the neutron spectrum from the $^7\text{Li}(p,n)$ reaction [11] arising from transitions to many-body final states. The measured $^7\text{Li}(p,n)$ spectrum shape was used to deconvolute the tail's contribution to the $\text{Se}(n,p)$ spectra. The procedure [11] is straightforward and has little effect at low excitation, but leads to about a 30% reduction in the number of counts at 30 MeV excitation. The results of a multipole decomposition analysis are also shown in Fig. 3. This analysis is discussed in the next section.

IV. CROSS-SECTION RESULTS

It is clear from these plots that no discrete states are strongly excited in the region of excitation shown. An attempt has been made to estimate the distribution of the GT strength using a multipole decomposition analysis [39]. In this analysis it is assumed that the cross section at each angle

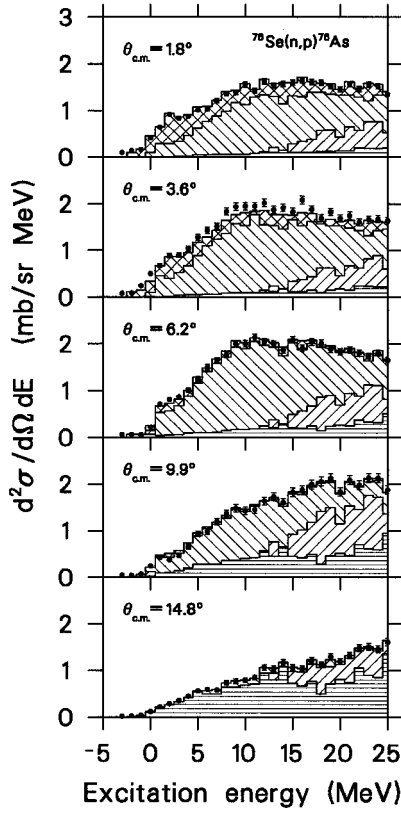


FIG. 3. The $\text{Se}(n,p)$ spectrum obtained at each MRS angle setting after background subtraction (solid points), and the results of the multipole decomposition analysis (hatched regions). Corrections have been applied to the spectra to account for the variation of the MRS acceptance across the focal plane and for the effects of a continuum in the neutron spectrum from the ${}^7\text{Li}(p,n)$ reaction. The cross hatched region corresponds to $\Delta L=0$, left hatched to $\Delta L=1$, right hatched to $\Delta L=2$, and horizontal hatched to $\Delta L=3$. See text for further explanation.

is an incoherent sum of contributions with different spin and parity transfers

$$\left[\frac{d\sigma}{d\Omega} \right]_{\text{exp}} = \sum_{\Delta J^\pi} C_{\Delta J^\pi} \left[\frac{d\sigma}{d\Omega} \right]_{\text{DW}}. \quad (5)$$

The theoretical angular distributions used in this expression are assumed to be given by calculations using the distorted wave impulse approximation (DWIA).

The sum should run over all ΔJ^π transfers consistent with the initial and final states, but since only five angles were measured, at most four values can be used. With this restriction, only those transition amplitudes that are expected to be the most important are chosen. In previous, similar analyses of (n,p) reactions on ${}^{51}\text{V}$ and ${}^{59}\text{Co}$ [15], it was found that the calculated angular distributions were sensitive mainly to the ΔL of the transition, and there was a much smaller variation with ΔJ for a given ΔL . In addition, simple particle-hole excitations were used to describe each transition amplitude [15]. In the present case, the specific choices were for $\Delta L=0$: $[\pi(p_{3/2})^{-1}, \nu(p_{1/2})^1]_{J^\pi=1^+}$, for $\Delta L=1$: $[\pi(f_{7/2})^{-1}, \nu(g_{9/2})^1]_{J^\pi=1^-}$, for $\Delta L=2$: $[\pi(p_{3/2})^{-1}, \nu(p_{1/2})^1]_{J^\pi=2^+}$, and for $\Delta L=3$: $[\pi(f_{5/2})^{-1}, \nu(g_{9/2})^1]_{J^\pi=3^-}$.

Other plausible choices might be expected to lie at higher excitation or to have a small amplitude because the level considered has a low occupation probability. The same choices for $\Delta L=0,1,2$ were made in a recent analysis of the ${}^{70,72}\text{Ge}(n,p)$ reactions [14]; the only difference here is that a $\Delta L=3$ contribution has been included separately rather than summing it in with the $\Delta L=2$ contribution.

The computer program DW81 [40] was used for the DWIA calculations. They were carried out in the same manner as previously [10–18,41]. Briefly, optical potentials for the distortions in DW81 were generated using the code MAINX8 [42], which folded an effective interaction with a three-parameter Fermi matter distribution. The Franey-Love interaction [43] was used for the effective interaction; it was also used in DW81. Harmonic oscillator functions with radius parameter $b=1.9$ fm were used for the single-particle wave functions. The calculations were carried out at 10 MeV intervals spanning the region of excitation from -5 to 35 MeV. The angular distributions for each 1 MeV energy bin were then obtained by interpolation.

The results are shown in Fig. 3. It can be seen in the fit to the 1.8° data that there is a small concentration of GT strength centered at ≈ 2 MeV excitation, with a nearly constant continuum extending above 6 MeV. The integrated GT cross section for the 1.8° data is 3.1 ± 0.1 mb/sr below 6 MeV excitation and 4.9 ± 0.2 mb/sr below 10 MeV excitation. It has been noted in previous analyses [15,41] using this procedure that the extraction of the $\Delta L=0$ (GT) strength becomes uncertain at energies where other multipoles, particularly $\Delta L=1$ (spin dipole), are dominant. The reason is that the shape of the spin dipole angular distribution is quite sensitive to the details of the distorted-wave calculation. In particular, different choices of distorting potential or particle-hole configuration for the transition can change the ratio between its value at 6° , near the peak, to that at 0° by up to 50% [12,15]. Based on this observation, the continuum of GT strength above 6 MeV is subject to a large uncertainty — beyond this energy the spin dipole contribution is clearly dominant.

In an attempt to extract the GT strength unencumbered by DWIA uncertainties, a second estimate of the distribution was obtained. The procedure is based on one suggested by Goodman and Bloom [44] in which the non-GT background in the 0° data was estimated from data at a nearby angle. Here a modified procedure [14] is followed that takes advantage of the fact that the $\Delta L=0$ cross section falls rapidly between 0° and 6° , whereas the $\Delta L=1$ cross section varies much more slowly. An estimate of the $\Delta L=1$ contribution to the cross section measured at 0° is then made by normalizing the measured 6° cross section to the measured 0° cross section at an excitation energy near the peak of the $\Delta L=1$ distribution calculated in the multipole decomposition analysis ($E_x \approx 10$ MeV was used), and subtracting the former from the latter.

This approach is likely to underestimate the GT strength. Part of the strength at 6° is still GT, and therefore some of the GT strength in the 0° spectrum will be removed by the subtraction. In addition, any GT strength that has the same distribution in excitation energy as the spin dipole will be missed [14]. Further, the method can be used to estimate the background in only the low excitation energy part of the

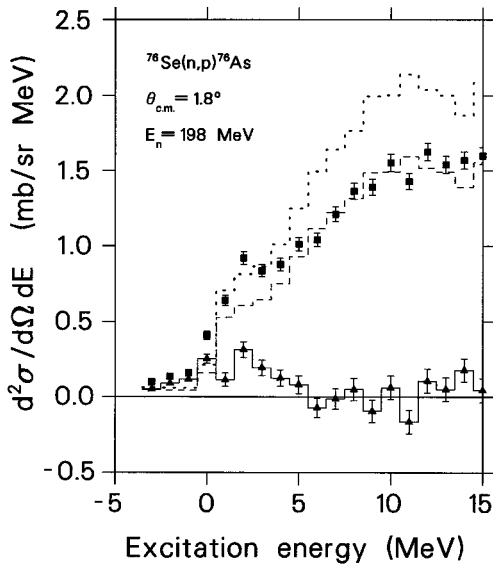


FIG. 4. Determination of the $\Delta L=0$ component of the $^{76}\text{Se}(n,p)^{76}\text{As}$ reaction at 1.8° using the 6° data to approximate the $\Delta L=1$ component. The squares are the 1.8° cross sections. The short dashed histogram is the 6.2° data, and the long dashed histogram is the 6.2° data after normalization to the 1.8° data at $E_x \approx 10$ MeV. The solid histogram and triangles show the 1.8° data after subtracting the normalized 6.2° data.

spectrum, since other multipolarities are also present and the procedure makes no allowance for them [45]. However, the technique should provide a reasonable estimate of the lower limit of the GT strength.

The result of the subtraction is shown in Fig. 4, and the integrated cross section for $E_x \leq 10$ MeV excitation is 1.1 ± 0.2 mb/sr. The error assigned is based on the facts that the $\Delta L=0$ cross section at 6° is still several percent of the 0° cross section, and that small differences would arise from choosing a different excitation energy for normalization. It is evident from Fig. 4 that with this method, the $\Delta L=0$ cross section is essentially zero above $E_x = 5$ MeV. It should also be noted that the integrated cross section is several times smaller than that found using the multipole decomposition.

In a previous analysis [14] comparing these two methods, a quite satisfactory agreement was found in the case of $^{70}\text{Ge}(n,p)$, but a result similar to the present one was found for $^{72}\text{Ge}(n,p)$; namely, the 6° subtraction method gave an integrated strength several times smaller than the multipole decomposition. The situation for the $^{76}\text{Se}(n,p)$ reaction is similar to that for the $^{72}\text{Ge}(n,p)$ reaction in that there is no strong state on which to base the normalization for the subtraction. The two reactions are also similar in that the spin dipole transition apparently already dominates the GT at an excitation energy of 6 MeV, and it has been noted above that a large uncertainty must then be associated with the GT strength extracted above this energy. The most reasonable approach might be to treat the result of the multipole decomposition as a best estimate with, however, a large uncertainty, and the result of the subtraction method as a lower limit.

V. GAMOW-TELLER STRENGTH

Cross sections measured in charge exchange reactions have been calibrated against the strength of known β decays

[5,11]. In the mass region pertinent to this experiment, the ratio of $\sigma(q=\omega=0)/B(\text{GT})=4.6$ mb/sr [5], where q is the momentum transfer and ω the energy transfer. For even- A targets of mass $A \leq 60$, the differences between empirically determined and calculated ratios vary by about 10% [5]. For $A > 60$, there are only four transitions for which both the (p,n) cross section and the β -decay strength have been measured, and three of these experimentally determined σ/B ratios agree within statistics with the calculated ratios.

Because of the finite angular resolution of the MRS and the nonzero Q value of the reaction, it was necessary to extrapolate the results of the measurement at 1.8° to $q=\omega=0$ before $B(\text{GT})$ could be extracted. The DWIA was used to extrapolate each 1 MeV energy bin, and it was found that $\sigma(q=\omega=0)/\sigma(1.8^\circ)$ varied from 1.2 to 1.6 over the lowest 10 MeV of excitation. The result for the analysis using the multipole decomposition was that the $\Delta L=0$ cross section at $q=\omega=0$ was corrected to 4.0 ± 0.2 mb/sr for $E_x \leq 6$ MeV, and to 6.7 ± 0.3 mb/sr for $E_x \leq 10$ MeV. For the analysis using the 6° subtraction method, the cross section was corrected to 1.6 ± 0.2 mb/sr for $E_x \leq 6$ MeV. Using the calibration above, the multipole decomposition results imply that $B(\text{GT}) = 0.86 \pm 0.03$ for $E_x \leq 6$ MeV and 1.45 ± 0.07 for $E_x \leq 10$ MeV, while the 6° subtraction results imply $B(\text{GT}) = 0.35 \pm 0.06$ for $E_x \leq 6$ MeV.

VI. MODEL COMPARISON

The distribution of $B(\text{GT})$ strength extracted from these measurements can be compared with calculations of the distribution. Here a comparison is made with a QRPA calculation based on the model of Engel, Vogel, and Zirnbauer [46]. Good agreement was found between this model and the results of measurements of the $^{54}\text{Fe}(n,p)^{54}\text{Mn}$ and $^{54}\text{Fe}(p,n)^{54}\text{Co}$ reactions [11]. Less satisfactory agreement was found with the measurements of the $^{70,72}\text{Ge}(n,p)$ reactions [14], although the location of the strength in $^{70}\text{Ge}(n,p)$ was well represented. A comparison with the results of the present multipole decomposition is shown in Fig. 5(a) for a calculation which used the lower limit for the strength of the particle-particle force (case a , $g^{\text{pp}}=130$), and in Fig. 5(b) for a calculation which used the upper limit (case b , $g^{\text{pp}}=144$). The limits were established from a comparison of calculated and measured β^+ -decay rates of semimagic nuclei [46]. The locations of the 1^+ states in the calculation are normally shifted so that the first state lies at the same energy as the first state observed experimentally [47]. In the present measurements in which there is no state strongly excited, the calculated states for case a have been shifted so that the first 1^+ state lies at the same excitation energy as the maximum strength extracted from the analysis. The locations of the calculated states have not been shifted for case b ; the calculated states are all weak and the first three lie near the maximum of the extracted strength in any event. Similar plots are shown in Figs. 6(a) and 6(b) for the results using the 6° background subtraction technique. The calculated peaks have not been shifted in these latter figures.

The multipole decomposition results show more total strength than either calculation (0.7 units for case a and 0.2 units for case b , for $E_x \leq 10$ MeV), while the 6° background subtraction result lies between the two calculated values. The

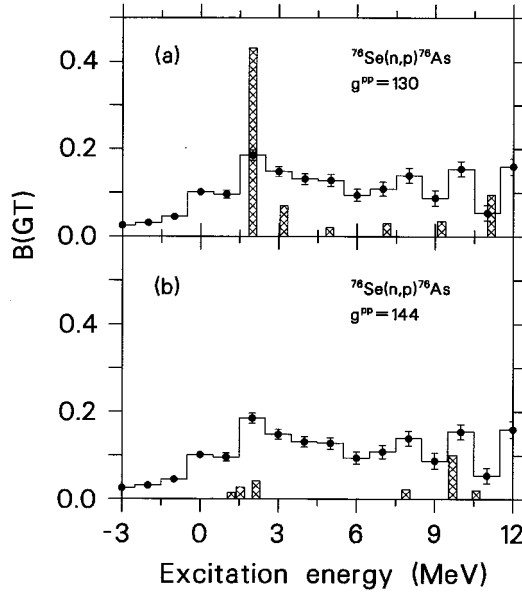


FIG. 5. (a) Comparison of the results of the multipole decomposition analysis with a QRPA calculation of the GT strength using the lower limit of the strength of the particle-particle force ($g^{\text{pp}}=130$). (b) Same as (a), but using the upper limit for g^{pp} .

results from the multipole decomposition analysis are unusual in that in most previous cases the experimentally measured values of $B(\text{GT})$ are quenched relative to calculated values rather than enhanced [3,11,14,18,48]. No quantitative conclusions are drawn because of the uncertainties associated with the present analysis.

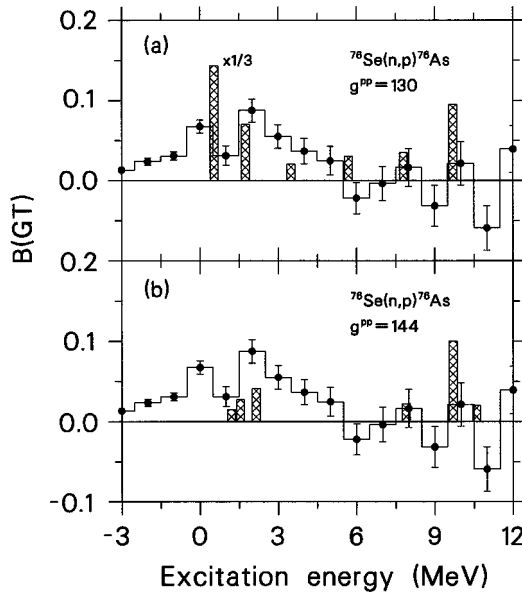


FIG. 6. (a) Comparison of the results of the analysis using the 6° background subtraction technique with a QRPA calculation of the GT strength using the lower limit of the strength of the particle-particle force ($g^{\text{pp}}=130$). (b) Same as (a), but using the upper limit for g^{pp} .

VII. LIFETIME FOR $2\nu\beta\beta$ DECAY OF ^{76}Ge

There have been four positive results reported from measurements of the $2\nu\beta\beta$ decay of ^{76}Ge [21,22,25,26]. The two most recent results are in mild disagreement; a collaboration between the PNL-USC and the ITEP-Yerevan groups [25] found $T_{1/2}^{2\nu} = 9.2_{-0.4}^{+0.7} \times 10^{20}$ y, while in a much higher statistics experiment the Heidelberg-Moscow group [26] found $T_{1/2}^{2\nu} = 14.2 \pm 0.3(\text{stat}) \pm 1.3(\text{syst}) \times 10^{20}$ y. Early shell-model calculations of the lifetime ranged from 2.2×10^{20} y [49] to 2.3×10^{21} y [50]. A more recent estimate, based on a calculation using the QRPA [46], ranged from 1.5×10^{20} y to 1.3×10^{21} y. This was the same calculation with which the $B(\text{GT})$ strength extracted from the present measurements was compared in the previous section, and the lifetime estimates correspond to the same limits of the particle-particle force.

It is possible to combine the results of the measurements on the $^{76}\text{Se}(n,p)^{76}\text{As}$ reaction reported here with those of the $^{76}\text{Ge}(p,n)^{76}\text{As}$ reaction [51] to estimate the value of the matrix element, $M_{2\nu}$, of Eq. (2). Such a calculation is subject to a large uncertainty, partly because although the GT strength distributions measured in (p,n) and (n,p) reactions provide measures of the magnitudes of the matrix elements in Eq. (2), the signs are not determined and cancellations among contributions at different energies could be important. In addition, the strength is measured over only a limited range of excitation energies. Finally, the energy resolution in the present study is not sufficient to allow unambiguous identification of transitions to specific states in the intermediate nucleus. Nevertheless, the principle of the comparison that can be made is outlined below.

The study of the $^{76}\text{Ge}(p,n)^{76}\text{As}$ reaction [51] identified several 1^+ states in ^{76}As up to an excitation of 15 MeV. It is not possible to identify these specific levels in the present work; instead the GT strengths extracted by both the multipole decomposition analysis and 6° subtraction analysis were fitted with a series of peaks located at the same excitation energies as were observed in the (p,n) measurements. The shape of each peak was taken to be a Gaussian with a width fixed by the energy resolution of the experiment (FWHM = 1.8 MeV).

In the case of the multipole decomposition analysis, an initial fit indicated that inclusion of the second excited state at 0.99 MeV was unnecessary; the error exceeded the magnitude of the fitted strength for this state. With this state excluded but with an extra state included whose location was left free, a satisfactory fit was obtained and is shown in Fig. 7(a). The free state was found to lie at 10.1 MeV excitation; there is no corresponding state from the (p,n) measurements at this energy. The value of the matrix element $M_{2\nu}$ from Eq. (2) was then found to be 0.16 under the assumptions that (i) the 0.99 MeV state is seen in the (p,n) reaction but not the (n,p) , (ii) the mixed state observed at 1.72 MeV and the broad peaks observed at 5.48 and 8.06 MeV in the (p,n) reaction are all pure 1^+ states, and (iii) the individual matrix elements all have the same sign. The phase-space factor of Eq. (1) has been calculated to be $5.2 \times 10^{-20} \text{ y}^{-1}$ [46]. Combined with the results of the (p,n) and (n,p) measurements, this leads to a decay rate of $1.4 \times 10^{-21} \text{ y}^{-1}$ and a half-life of $T_{1/2}^{2\nu} = 7.4 \times 10^{20}$ y.

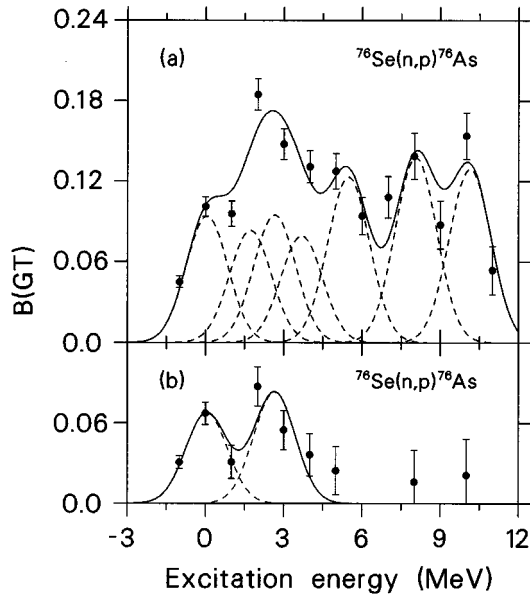


FIG. 7. Fits to the Gamow-Teller strength assuming transitions to 1^+ states in ^{76}As seen in $^{76}\text{Ge}(p,n)$. The data are represented by the solid points. The solid curves through the data are the sums of the peaks shown (dashed lines). (a) Fit for the multipole decomposition analysis. (b) Fit for the 6° subtraction analysis.

A satisfactory fit to the spectrum extracted with the 6° subtraction analysis was obtained by including only the states observed at 0.05 and 2.65 MeV in the (p,n) measurements. This fit is shown in Fig. 7(b). Inclusion of any other states led either to a much higher chi-squared for the fit or to strengths for the extra states whose uncertainties exceeded the magnitudes. The value of $M_{2\nu}$ was then found to be 0.047 with the assumptions that no states other than these two are excited in the (n,p) reaction and that the individual matrix elements all have the same sign. The decay rate is found to be $1.2 \times 10^{-22} \text{ y}^{-1}$ and the half-life to be $T_{1/2}^{2\nu} = 8.7 \times 10^{21} \text{ y}$.

The value for the half-life estimated from the multipole decomposition analysis is slightly shorter than, but within a factor of 2 of, the experimental results [25,26]. The agree-

ment could be improved by relaxing assumptions (ii) and (iii) above. The half-life estimated from the 6° subtraction analysis is considerably longer than that measured. Taking this result at face value would imply that there must be states lying at higher excitation which also contribute to the decay. The nature of the analysis technique precludes the possibility of uncovering any such strength. In this context, it should also be noted that it has been suspected for some time [52], and more systematically argued in recent years [53,54], that only a few low-lying excitations should contribute to the $2\nu \beta\beta$ -decay matrix element. The arguments center around the idea that any high-lying strength will contribute to $M_{2\nu}$ with random signs, and so will tend to cancel out. Unfortunately the data presented here are not sufficiently quantitatively precise for a definite statement to be made.

VIII. CONCLUSIONS

Gamow-Teller strength excited in the $^{76}\text{Se}(n,p)^{76}\text{As}$ reaction at 198 MeV has been measured. This reaction acts as a probe of transitions important in the $2\nu \beta\beta$ decay of ^{76}Ge ; the data are useful as a check of calculations of the rate for this decay. Although a small concentration of GT strength has been found below 6 MeV excitation, its distribution above this energy is uncertain because of its weakness relative to other modes of excitation. Even below 6 MeV, two plausible methods of extracting the strength disagree quantitatively by more than a factor of 2. Hence these results must be considered to be of a qualitative nature only.

Nevertheless, the data presented here provide a challenge for rapidly improving shell-model calculations in the fp shell [55–58]. In this respect, it is a continuation of studies of other fp shell nuclei [11–16,59]. Whether the small β^+ strengths in such heavy nuclei can be reproduced without an *ad hoc* renormalization, for example, of the nucleon's axial coupling constant, remains an open question.

ACKNOWLEDGMENTS

This work was supported in part by a grant from the Natural Sciences and Engineering Research Council of Canada.

-
- [1] T. N. Taddeucci, J. Rapaport, D. E. Bainum, C. D. Goodman, C. C. Foster, C. Gaarde, J. Larsen, C. A. Goulding, D. J. Horen, T. Masterson, and E. Sugarbaker, *Phys. Rev. C* **25**, 1094 (1982).
 - [2] W. P. Alford, R. L. Helmer, R. Abegg, A. Celler, O. Häusser, K. Hicks, K. P. Jackson, C. A. Miller, S. Yen, R. E. Azuma, D. Frekers, R. S. Henderson, H. Baer, and C. D. Zafiratos, *Phys. Lett. B* **179**, 20 (1986).
 - [3] C. D. Goodman, C. A. Goulding, M. B. Greenfield, J. Rapaport, D. E. Bainum, C. C. Foster, W. G. Love, and F. Petrovich, *Phys. Rev. Lett.* **44**, 1755 (1980).
 - [4] K. P. Jackson, A. Celler, W. P. Alford, K. Raywood, R. Abegg, R. E. Azuma, C. K. Campbell, S. El-Kateb, D. Frekers, P. W. Green, O. Häusser, R. L. Helmer, R. S. Henderson, K. H. Hicks, R. Jeppesen, P. Lewis, C. A. Miller, A. Moalem, M. A. Moinester, R. B. Schubank, G. G. Shute, B. M. Spicer, M. C. Vetterli, A. I. Yavin, and S. Yen, *Phys. Lett. B* **201**, 25 (1988).
 - [5] T. N. Taddeucci, C. A. Goulding, T. A. Carey, R. C. Byrd, C. D. Goodman, C. Gaarde, J. Larsen, D. Horen, J. Rapaport, and E. Sugarbaker, *Nucl. Phys.* **A469**, 125 (1987).
 - [6] D. E. Bainum, J. Rapaport, C. D. Goodman, D. J. Horen, C. C. Foster, M. B. Greenfield, and C. A. Goulding, *Phys. Rev. Lett.* **44**, 1751 (1980).
 - [7] C. Gaarde, J. Rapaport, T. N. Taddeucci, C. D. Goodman, C. C. Foster, D. E. Bainum, C. A. Goulding, M. B. Greenfield, D. J. Horen, and E. Sugarbaker, *Nucl. Phys.* **A369**, 258 (1981).
 - [8] D. Wang, J. Rapaport, D. J. Horen, B. A. Brown, C. Gaarde, C. D. Goodman, E. Sugarbaker, and T. N. Taddeucci, *Nucl. Phys.* **A480**, 285 (1988).

- [9] J. Rapaport, C. C. Foster, C. D. Goodman, C. A. Goulding, T. N. Taddeucci, D. J. Horen, E. R. Sugarbaker, C. Gaarde, J. Larsen, J. A. Carr, F. Petrovich, and M. J. Threapleton, *Phys. Rev. C* **41**, 1920 (1990).
- [10] M. C. Vetterli, O. Häusser, W. P. Alford, D. Frekers, R. Helmer, R. Henderson, K. Hicks, K. P. Jackson, R. G. Jeppesen, C. A. Miller, M. A. Moinester, K. Raywood, and S. Yen, *Phys. Rev. Lett.* **59**, 439 (1987).
- [11] M. C. Vetterli, O. Häusser, R. Abegg, W. P. Alford, A. Celler, D. Frekers, R. Helmer, R. Henderson, K. H. Hicks, K. P. Jackson, R. G. Jeppesen, C. A. Miller, K. Raywood, and S. Yen, *Phys. Rev. C* **40**, 559 (1989).
- [12] W. P. Alford, R. L. Helmer, R. Abegg, A. Celler, D. Frekers, P. Green, O. Häusser, R. Henderson, K. Hicks, K. P. Jackson, R. Jeppesen, C. A. Miller, A. Trudel, M. Vetterli, and S. Yen, *Nucl. Phys.* **A514**, 49 (1990).
- [13] W. P. Alford, A. Celler, B. A. Brown, R. Abegg, K. Ferguson, R. Helmer, K. P. Jackson, S. Long, K. Raywood, and S. Yen, *Nucl. Phys.* **A531**, 97 (1991).
- [14] M. C. Vetterli, K. P. Jackson, A. Celler, J. Engel, D. Frekers, O. Häusser, R. Helmer, R. Henderson, K. H. Hicks, R. G. Jeppesen, B. Larson, B. Pointon, A. Trudel, and S. Yen, *Phys. Rev. C* **45**, 997 (1992).
- [15] W. P. Alford, B. A. Brown, S. Burzynski, A. Celler, D. Frekers, R. Helmer, R. Henderson, K. P. Jackson, K. Lee, A. Rahav, A. Trudel, and M. C. Vetterli, *Phys. Rev. C* **48**, 2818 (1993).
- [16] S. El-Kateb, K. P. Jackson, W. P. Alford, R. Abegg, R. E. Azuma, B. A. Brown, A. Celler, D. Frekers, O. Häusser, R. Helmer, R. S. Henderson, K. H. Hicks, R. Jeppesen, J. D. King, K. Raywood, G. G. Shute, B. M. Spicer, A. Trudel, M. Vetterli, and S. Yen, *Phys. Rev. C* **49**, 3128 (1994).
- [17] K. J. Raywood, B. M. Spicer, S. Yen, S. A. Long, M. A. Moinester, R. Abegg, W. P. Alford, A. Celler, T. E. Drake, D. Frekers, P. E. Green, O. Häusser, R. L. Helmer, R. S. Henderson, K. H. Hicks, K. P. Jackson, R. G. Jeppesen, J. D. King, N. S. P. King, C. A. Miller, V. C. Officer, R. Schubank, G. G. Shute, M. Vetterli, J. Watson, and A. I. Yavin, *Phys. Rev. C* **41**, 2836 (1990).
- [18] A. Celler, S. Yen, W. P. Alford, R. Abegg, B. A. Brown, S. Burzynski, D. Frekers, O. Häusser, R. Helmer, R. S. Henderson, K. Hicks, K. P. Jackson, R. Jeppesen, C. A. Miller, M. A. Moinester, B. W. Pointon, A. Trudel, and M. C. Vetterli, *Phys. Rev. C* **47**, 1563 (1993).
- [19] T. Kirsten, E. Heusser, D. Kaether, J. Oehm, E. Pernicka, and H. Richter, in *Proceeding of the International Symposium on Nuclear Beta Decays and Neutrino*, edited by T. Kotani, H. Ejiri, and E. Takasugi (World Scientific, Singapore, 1986), p. 81; O. K. Manuel, *ibid.*, p. 71.
- [20] S. R. Elliott, A. A. Hahn, and M. K. Moe, *Phys. Rev. Lett.* **59**, 2020 (1987).
- [21] H. S. Miley, F. T. Avignone III, R. L. Brodzinski, J. I. Collar, and J. H. Reeves, *Phys. Rev. Lett.* **65**, 3092 (1990).
- [22] A. A. Vasenko, I. V. Kirpichnikov, V. A. Kuznetsov, A. S. Starostin, A. G. Djanyan, V. S. Pogosov, S. P. Shachysisyan, and A. G. Tamanyan, *Mod. Phys. Lett. A* **5**, 1299 (1990).
- [23] H. Ejiri, K. Fushimi, T. Kamada, H. Kinoshita, H. Kobiki, H. Ohsumi, K. Okada, H. Sano, T. Shibata, T. Shima, N. Tanabe, J. Tanaka, T. Taniguchi, T. Watanabe, and N. Yamamoto, *Phys. Lett. B* **258**, 17 (1991).
- [24] S. R. Elliott, M. K. Moe, M. A. Nelson, and M. A. Vient, *J. Phys. G* **17**, S145 (1991).
- [25] F. T. Avignone III, R. L. Brodzinski, C. K. Guerard, I. V. Kirpichnikov, H. S. Miley, V. S. Pogosov, J. H. Reeves, A. S. Starostin, and A. G. Tamanyan, *Phys. Lett. B* **256**, 559 (1991).
- [26] A. Balysh, M. Beck, S. T. Belyaev, F. Bensch, J. Bockholt, A. Demehin, A. Gurov, G. Heusser, H. V. Klapdor-Kleingrothaus, I. Kondratenko, D. Kotel'nikov, V. I. Lebedev, B. Maier, A. Müller, F. Petry, A. Piepke, A. Pronsky, H. Strecker, M. Völlinger, and K. Zuber, *Phys. Lett. B* **322**, 176 (1994).
- [27] W. C. Haxton, G. J. Stephenson Jr., and D. Strottman, *Phys. Rev. D* **25**, 2360 (1982); W. C. Haxton and G. J. Stephenson, Jr., *Prog. Part. Nucl. Phys.* **12**, 409 (1984).
- [28] T. Tsuboi, K. Muto, and H. Horie, *Phys. Lett. B* **143**, 293 (1984).
- [29] P. Vogel and M. R. Zirnbauer, *Phys. Rev. Lett.* **57**, 3148 (1986).
- [30] O. Civitarese, A. Faessler, and T. Tomoda, *Phys. Lett. B* **194**, 11 (1987).
- [31] K. Muto and H. V. Klapdor, *Phys. Lett. B* **201**, 420 (1988).
- [32] P. Vogel and P. Fisher, *Phys. Rev. C* **32**, 1362 (1985).
- [33] C. Gaarde, *Nucl. Phys.* **A396**, 127c (1983).
- [34] B. A. Brown, in *Nuclear Shell Models*, edited by M. Vallieres and B. H. Wildenthal (World Scientific, Singapore, 1985), p. 42.
- [35] R. Helmer, *Can. J. Phys.* **65**, 588 (1987).
- [36] R. S. Henderson, W. P. Alford, D. Frekers, O. Häusser, R. L. Helmer, K. H. Hicks, K. P. Jackson, C. A. Miller, M. C. Vetterli, and S. Yen, *Nucl. Instrum. Methods Phys. Res. A* **257**, 97 (1987).
- [37] MRS manual, TRIUMF (unpublished).
- [38] R. A. Arndt and L. D. Soper, "Scattering Analysis Interactive Dial-in (SAID) program (SM90)" (unpublished); R. A. Arndt, L. D. Soper, R. L. Workman, and M. W. McNaughton, *Phys. Rev. D* **45**, 3995 (1992).
- [39] M. A. Moinester, *Can. J. Phys.* **65**, 660 (1987).
- [40] R. Schaeffer and J. Raynal, Computer Code DWBA70 (unpublished); J. R. Comfort, Computer code DW81 (extended version of DWBA70), Arizona State University, 1984.
- [41] A. Celler, W. P. Alford, R. Abegg, D. Frekers, O. Häusser, R. Helmer, R. S. Henderson, K. P. Jackson, R. Jeppesen, B. Larson, J. Mildenerger, B. W. Pointon, A. Trudel, M. Vetterli, and S. Yen, *Phys. Rev. C* **43**, 639 (1991).
- [42] T. Cooper, Computer code MAINX8 (private communication); modified by R. G. Jeppesen (unpublished).
- [43] M. A. Franey and W. G. Love, *Phys. Rev. C* **31**, 488 (1985).
- [44] C. D. Goodman and S. D. Bloom, in *Spin Excitations in Nuclei*, edited by F. Petrovich, G. E. Brown, G. T. Garvey, C. D. Goodman, R. A. Lindgren, and W. G. Love (Plenum, New York, 1984), p. 143.
- [45] J. Rapaport, T. Taddeucci, T. P. Welch, C. Gaarde, J. Larsen, D. J. Horen, E. Sugarbaker, P. Koncz, C. C. Foster, C. D. Goodman, C. A. Goulding, and T. Masterson, *Nucl. Phys.* **A410**, 371 (1983).
- [46] J. Engel, P. Vogel, and M. R. Zirnbauer, *Phys. Rev. C* **37**, 731 (1988).
- [47] J. Engel, P. Vogel, O. Civitarese, and M. R. Zirnbauer, *Phys. Lett. B* **208**, 187 (1988).
- [48] J. Rapaport, in *The Interaction Between Medium Energy*

- Nucleons in Nuclei-1982*, edited by H. O. Meyer (AIP, New York, 1983), p. 365.
- [49] H. Primakoff and S. P. Rosen, *Phys. Rev.* **184**, 1925 (1969).
- [50] M. Doi, T. Kotani, H. Nishiura, and E. Takasugi, *Prog. Theor. Phys.* **69**, 602 (1983).
- [51] R. Madey, B. S. Flanders, B. D. Anderson, A. R. Baldwin, J. W. Watson, Sam M. Austin, C. C. Foster, H. V. Klapdor, and K. Grotz, *Phys. Rev. C* **40**, 540 (1989).
- [52] J. Abad, A. Morales, R. Nuñez-Lagos, and P. F. Pacheco, *Ann. Fis. A* **80**, 9 (1984).
- [53] Magda Ericson, Torleif Ericson, and Petr Vogel, *Phys. Lett. B* **328**, 259 (1994).
- [54] Hiroyasu Ejiri and Hiroshi Toki, *J. Phys. Soc. Jpn.* **65**, 7 (1996).
- [55] E. Caurier, A. Poves, and A. P. Zuker, *Phys. Lett. B* **252**, 13 (1990).
- [56] E. Caurier, A. P. Zuker, A. Poves, and G. Martínez-Pinedo, *Phys. Rev. C* **50**, 225 (1994).
- [57] K. Langanke, D. J. Dean, P. B. Radha, Y. Alhassid, and S. E. Koonin, *Phys. Rev. C* **52**, 718 (1995).
- [58] K. Langanke, D. J. Dean, P. B. Radha, and S. E. Koonin, *Nucl. Phys.* **A602**, 244 (1996).
- [59] A. L. Williams, W. P. Alford, E. Brash, B. A. Brown, S. Burzynski, H. T. Fortune, O. Häusser, R. Helmer, R. Henderson, P. P. Hui, K. P. Jackson, B. Larson, M. G. McKinzie, D. A. Smith, A. Trudel, and M. Vetterli, *Phys. Rev. C* **51**, 1144 (1995).